

Printed covalent glycan array for ligand profiling of diverse glycan binding proteins

Ola Blixt^{a,b,c}, Steve Head^d, Tony Mondala^d, Christopher Scanlan^e, Margaret E. Huflejt^f, Richard Alvarez^g, Marian C. Bryan^h, Fabio Fazio^h, Daniel Calarese^e, James Stevens^b, Nahid Razi^{a,b}, David J. Stevensⁱ, John J. Skehel^j, Irma van Die^j, Dennis R. Burton^{b,e}, Ian A. Wilson^b, Richard Cummings^g, Nicolai Bovin^k, Chi-Huey Wong^{a,h}, and James C. Paulson^{a,b}

^aGlycan Synthesis and Protein Expression Core-D, Consortium for Functional Glycomics, ^dDNA Microarray Core Facility, and Departments of ^bMolecular Biology, ^hChemistry, and ^eImmunology, The Scripps Research Institute, 10550 North Torrey Pines Road, La Jolla, CA 92037; ^fSidney Kimmel Cancer Center, 10835 Altman Row, San Diego, CA 92121; ^gDepartment of Biochemistry and Molecular Biology, University of Oklahoma Health Science Center, 975 NE 10th Street, BRC 411B, P.O. Box 26901, Oklahoma City, OK 73104; ⁱMedical Research Center National Institute for Medical Research, Mill Hill, London NW7, United Kingdom; ^jDepartment of Molecular Cell Biology and Immunology, Vrije Universiteit Medical Centre, 1007 MB, Amsterdam, The Netherlands; and ^kShemyakin and Ovchinnikov Institute of Bioorganic Chemistry, Russian Academy of Sciences, 16/10 Miklukho-Maklaya ul, Moscow, 117997, V-437, Russian Federation

Contributed by Chi-Huey Wong, October 26, 2004

Here we describe a glycan microarray constructed by using standard robotic microarray printing technology to couple amine functionalized glycans to an amino-reactive glass slide. The array comprises 200 synthetic and natural glycan sequences representing major glycan structures of glycoproteins and glycolipids. The array has remarkable utility for profiling the specificity of a diverse range of glycan binding proteins, including C-type lectins, siglecs, galectins, anticarbohydrate antibodies, lectins from plants and microbes, and intact viruses.

carbohydrate | lectin | microarray | glycoprotein | glycolipid

With 50% or more of all proteins carrying glycan chains, glycomics has emerged with proteomics as an area for development and exploration in the postgenomics era. As vital constituents of all living systems, glycans are involved in recognition, adherence, motility, and signaling processes (1, 2). Glycan binding proteins (GBPs) play a significant role in decoding the information content of glycans by recognizing and specifically binding to glycosylated protein and lipid ligands. However, the enormous complexity of GBP–ligand interactions and the absence of well defined glycan libraries and efficient analytical screening methods have limited analysis of their specificity and elucidation of their biological roles. To address these limitations, development of reliable and efficient tools for analysis of GBP specificity is needed.

In recent years, several approaches for construction of glycan arrays for analysis of GBP specificity (3–6) have emerged. Each format differs in the type of glycans and the manner in which they are displayed. Some use noncovalent attachment to plastic or nitrocellulose membrane (6–12), and others use covalent attachment to plastic, gold, or glass (6, 13–20). The glycans displayed range from a limited number of 5–45 exemplary structures representing terminal sequences on glycoprotein or glycolipid glycans (6, 7, 11–20), to libraries of defined glycans, proteoglycan fragments, and microbial polysaccharides (8–10).

In this article we describe a glycan array format that uses standard robotic printing technology for the creation of a diverse glycan array with demonstrated applicability for profiling the specificity of a wide variety of GBPs. This array uses commercially available amine-reactive *N*-hydroxysuccinimide (NHS)-activated glass slides, which allow rapid covalent coupling of amine-functionalized glycans or glycoconjugates. Advantage was taken of the existence of a glycan library comprising >200 synthetic and natural structurally defined terminal sequences of glycoprotein and glycolipid glycans¹ developed for an ELISA-based array (8), which could be readily modified to contain amino-functionalized linkers for covalent coupling to NHS-activated glass slides. We demonstrate the utility of this array for

analysis of most major classes of GBPs, including mammalian lectins (C-type lectins, galectins, and siglecs), plant lectins, antibodies, viral and bacterial lectins, and intact viruses.

Materials and Methods

Materials. Natural glycoproteins, α -acid glycoprotein (α_1 -AGP) and α_1 -AGP glycoform A and B **1–3**, were prepared as described (21). Ceruloplasmin **4**, fibrinogen **5**, and apo-transferrin **6** were from Sigma-Aldrich. Synthetic glycan ligands **7–134** and **146–200** were prepared or obtained as described (22–26) or were from The Consortium for Functional Glycomics (<http://functionalglycomics.org>). Ligands **111** and **135–139** were obtained through one-pot chemical synthesis as described (27). Ligands **140–145** were isolated from ribonuclease as described in *Supporting Methods*, which is published as supporting information on the PNAS web site. NHS-activated glass slides (Slide-H) were from Schott Nexterion (Mainz, Germany), and the robotic printing arrayer was custom-made by Robotic Labware Designs (Carlsbad, CA). Arrays were printed by using CMP4B microarray spotting pins (TeleChem International, Sunnyvale, CA). GBPs were obtained from commercial sources [Con A and *Erythrina cristagalli* (ECA) from EY Laboratories and anti-CD15 from BD Biosciences, San Jose, CA] or supplied by investigators [dendritic cell-specific intercellular adhesion molecule-1-grabbing nonintegrin (DC-SIGN) (28), influenza virus A/Puerto Rico/8/34 (H1N1) (29), 2G12 (30), cyanovirin-N (CVN) (31), and H3 hemagglutinin (J.S. and I.A.W.)]. Human serum was obtained from healthy volunteers at The General Clinical Research Center, Scripps Hospital, La Jolla, CA. The samples were centrifugated for 30 min at 1,500 \times *g* and heat-inactivated at 56°C for 25 min. CD22 was expressed and purified as described (32). Recombinant human galectin-4 was prepared as described for rat galectin-4 by Huflejt *et al.* (33). Galectin-4-Alexa Fluor 488 was made with an Alexa Fluor 488 protein labeling kit from Molecular Probes according to the manufacturer's instruction. Rabbit anti-CVN was obtained as described (31), and monoclonal mouse anti-human-IgG-IgM-IgA-biotin antibody and streptavidin-FITC were from Pierce. Rabbit anti-goat-IgG-FITC, goat anti-human-IgG-FITC, mouse anti-HisTag-IgG-Alexa Fluor 488, and anti-mouse-IgG-Alexa Fluor 488 were

Freely available online through the PNAS open access option.

Abbreviations: CVN, cyanovirin-N; DC-SIGN, dendritic cell-specific intercellular adhesion molecule-1-grabbing nonintegrin; ECA, *Erythrina cristagalli*; GBP, glycan binding protein; NHS, *N*-hydroxysuccinimide.

[†]To whom correspondence should be addressed. E-mail: olablixt@scripps.edu.

¹Compound library was produced by the Consortium for Functional Glycomics (www.functionalglycomics.org).

© 2004 by The National Academy of Sciences of the USA

Table 1. Valency of GBPs analyzed with the glycan array

Category	GBP	Valency	2° Ab	3° Ab	Final
Plant lectin	Con A-FITC	4			4
Plant lectin	ECA-FITC	2			2
Human C type	DC-SIGN-Fc*	2			2
Human siglec	CD22-Fc	2	α-hlgG-F	α-glgG-F	8
Human galectin	Galectin-4-AF488	2			2
Human IgG	Anti-CD15-FITC	2			2
Human IgG	2G12	2	α-hlgG-AF		4
Human IgG/A/M	Serum†	2			2
Bacterial GBP	Cyanovirin‡	2			2
Viral GBP	Influenza HA (H3)	3	α-HA-AF	α-mlgG-AF	12
Intact virus	Influenza (PR8) [§]	500	α-PR8	α-rlgG-AF	500

Ab, antibody; F, FITC; AF, Alexa Fluor 488; HA, hemagglutinin.

*After binding of DC-SIGN, binding was detected by overlay with anti-human IgG-AF488.

†After binding of serum diluted 1:25 with PBS, binding was detected by overlay with goat anti-human IgG/M/A-Biotin (1:100) (Pierce) followed by streptavidin-FITC (1:100).

‡After binding of CVN, binding was detected by overlay with polyclonal rabbit anti-CVN IgG-AF488 followed by anti-rabbit-IgG-FITC.

§After binding of virus, binding was detected by overlay with rabbit anti-PR8 followed by goat anti-rabbit-IgG-AF488.

purchased from Vector Laboratories. Rabbit anti-influenza virus A/PR/8/34 was from the World Influenza Centre, London. Other reagents and consumables were from commercial sources with highest possible quality.

Glycan Array Fabrication. Microarrays were printed by robotic pin deposition of ≈ 0.6 nl of various concentrations of amine-containing glycans in print buffer (300 mM phosphate, pH 8.5 containing 0.005% Tween-20) onto NHS-activated glass slides. Each compound was printed at two concentrations (100 and 10 μ M), and each concentration was used in a replicate of six. Printed slides were allowed to react in an atmosphere of 80% humidity for 30 min followed by desiccation overnight. Remaining NHS groups were blocked by immersion in buffer (50 mM ethanolamine in 50 mM borate buffer, pH 9.2) for 1 h. Slides were rinsed with water, dried, and stored in desiccators at room temperature before use.

GBP Binding Assay. Printed slides were analyzed without any further modification of the surface. Slides were incubated in either a one-step procedure with labeled proteins or a sandwich procedure in which the bound GBP was overlaid with labeled secondary antibodies or GBPs precomplexed with labeled antibodies. GBPs were added at a concentration of 5–50 μ g/ml in buffer (usually PBS containing 0.005–0.5% Tween-20). Secondary antibodies (10 μ g/ml in PBS) were overlaid on bound GBP. GBP-antibody precomplexes were prepared in a molar ratio of 1:0.5:0.25 (5–50 μ g/ml) for GBP/2° antibody/3° antibody, respectively (15 min on ice). The samples (50–100 μ l) were applied either directly onto the surface of a single slide and covered with a microscope coverslip or applied between two parallel slides separated by thin tape and pressed together by paper clips (34) and then incubated in a humidified chamber for 30–60 min. Slides were subsequently washed by successive rinses in (i) PBS-0.05% Tween, (ii) PBS, and (iii) deionized water, then immediately subjected to imaging. Serum samples were typically used at dilutions of 1:25, and 0.4–0.8 ml was applied directly onto the slide surface without any cover glass. The slides were gently rocked at room temperature for 90 min followed by detection with secondary antibodies (Table 1). Whole virus was applied (0.8 ml) at a concentration of 100 μ g/ml in buffer (PBS containing 0.05% Tween-20) containing the neuraminidase inhibitor oseltamivir carboxylate (10 μ M). The slides were gently rocked at room temperature for 90 min followed by detection

with secondary antibodies in the presence of the neuraminidase inhibitor (Table 1).

Image Acquisition and Signal Processing. Fluorescence intensities were detected by using a ScanArray 5000 (PerkinElmer) confocal scanner, and image analyses were carried out by using IMAGENE image analysis software (BioDiscovery, El Segundo, CA). Signal-to-background was typically $>50:1$, and no background subtractions were performed. Data were plotted by using Microsoft EXCEL software.

Results

Glycan Array Design. We adopted a strategy for covalently attaching a defined glycan library to microglass slides by using standard microarray printing technology (Fig. 1). The use of an amino-reactive NHS-activated microglass surface allows covalent attachment of glycans containing a terminal amine by forming an amide bond under aqueous conditions at room temperature. The compound library of 200 glycoconjugates comprises diverse and biologically relevant structures representing terminal sequences of glycoprotein and glycolipid glycans (see *Methods* and *Supporting Methods*)¹ (22–26, 35). Glycan structures detected by GBPs analyzed in this article are listed in Fig. 2, and a complete glycan listing is provided in Fig. 7, which is published as supporting information on the PNAS web site. In addition, exemplary symbol structures summarizing the principal specificities of each GBP are depicted in each figure.

Optimization of Glycan Printing. Length of time of the printing process was a concern because the moisture-sensitive NHS slides would be exposed to air during the procedure. Binding of fluorescein-labeled Con A was used as a measure of ligand coupling. Maximal binding of Con A to high mannose glycans, **134–138**, was obtained at concentrations >50 μ M, with $<10\%$ variation in maximal binding observed with printing times up to 5 h, as shown in Fig. 3A for compound **136**. For the complete array, standard printing concentrations of 100 and 10 μ M of each glycan were selected to represent saturating and subsaturating levels, respectively, of the printed glycan. All samples were printed in replicates of six to generate an array of $>2,400$ spotted ligands per glass slide, including controls.

General Approach for Profiling GBP Specificity. In general, GBPs have low affinity for their ligands and would not be expected to

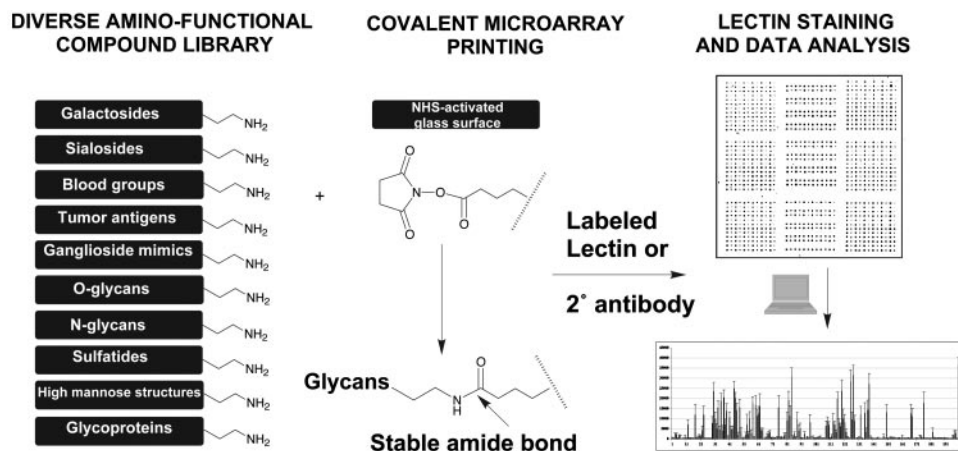


Fig. 1. Covalent printing of a diverse glycan library onto an amino-reactive glass surface and image analysis by using standard microarray technology.

bind with sufficient avidity to withstand washing steps to remove unbound protein (36). For this reason, our routine approach is to create multivalency as necessary to mimic the multivalent interactions that occur in nature. GBPs evaluated here and the degree of multivalency used to achieve robust binding is summarized in Table 1. The valency required for binding ranged from 2 to 12. In several cases monovalent GBPs were evaluated as divalent recombinant Ig-Fc chimeras, and in others higher valency was achieved through the use of secondary antibodies. Binding was detected by including a fluorescent label either on the GBP or secondary antibody.

Specificity of Plant Lectins. As shown in Fig. 3B, two lectins, Con A and ECA, exhibited binding to different subsets of glycans on the array, consistent with their reported specificities. Con A bound selectively to synthetic ligands consisting of one or more α -D-mannose (Man α 1) residues and to isolated high-mannose N-glycans, and a biantennary N-linked glycan (134-145 and 199). ECA bound exclusively to various terminal N-acetyllactosamine (LacNAc) structures, polyLacNAc (9, 73, and 76), and branched O-glycans (49 and 72). ECA also tolerated terminal Fuc α 1-2Gal substitution (105-107). These specificities are consistent with those previously observed by using other methodologies (37-40).

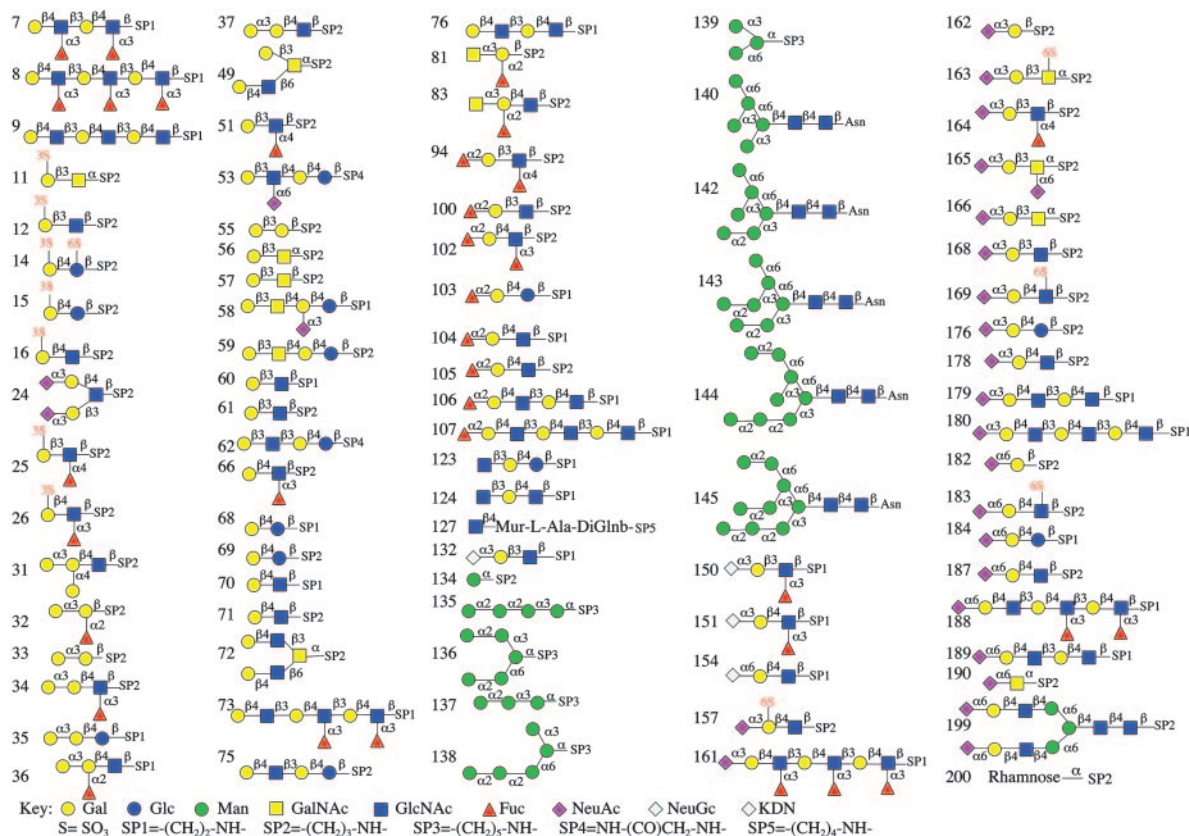


Fig. 2. Representative glycan structures on the array. Glycan structures detected by GBPs in this article are shown in the symbol nomenclature adopted by the Consortium for Functional Glycomics (www.functionalglycomics.org). A full list of glycans can be found in Fig. 7.

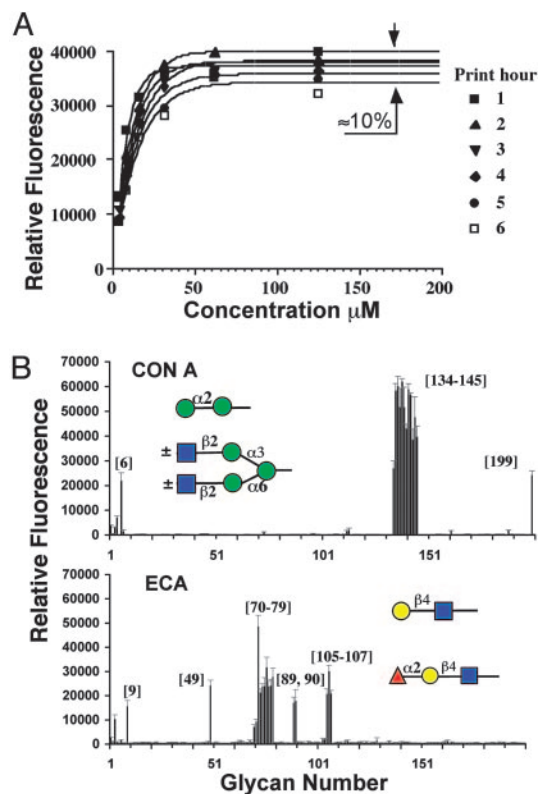


Fig. 3. Printing optimization and specificity of selected plant lectins. (A) Optimization of glycan concentration and length of printing time were determined by printing mannose structures and detected by Con A. A representative mannose glycan (136) was printed at various concentrations (4–500 μM) in replicates of eight at six different time points. (B) Binding specificities of Con A-FITC and ECA-FITC on the complete array.^m

Analysis of Specificities of Human GBPs. Three major families of mammalian GBPs are involved in cell surface biology through recognition of glycan ligands: C-type lectins, siglecs, and galectins. One exemplary member from each class was selected for analysis (Fig. 4).

DC-SIGN, a member of the group 2 subfamily of the C-type lectin family, is a dendritic cell protein implicated in innate immunity and the pathogenicity of HIV-1 (41). As shown in Fig. 4, a recombinant DC-SIGN-Fc recognized two classes of glycans, various fucosylated oligosaccharides with the $\text{Fu}\alpha\text{1-3GlcNAc}$ and $\text{Fu}\alpha\text{1-4GlcNAc}$ oligosaccharides found as terminal sequences on N- and O-linked oligosaccharides (7, 8, 51, 66, 94, and 102), and mannose-containing oligosaccharides terminated with $\text{Man}\alpha\text{1-2-residues}$ (135–138, 144, and 145), consistent with specificities found by other groups (8, 28, 42).

CD22, a member of the Ig superfamily lectins (Siglecs), is a well known negative regulator of B cell signaling and binds selectively to glycans with $\text{Sia}\alpha\text{2-6Gal-}$ sequences (32, 43–45). CD22 bound exclusively to the seven structures containing the terminal $\text{Sia}\alpha\text{2-6Gal}\beta\text{1-4GlcNAc-}$ sequence including a bi-antennary N-linked glycan (154, 187–189, and 199). An additional 6-O-GlcNAc sulfation ($\text{Neu5Ac}\alpha\text{2-6Gal}\beta\text{1-4[6Su]GlcNAc-}$ 183) appeared to enhance binding relative to the corresponding nonsulfated glycan, suggesting that this glycan could be a preferred ligand for human CD22.

Galectins are a family of β -galactoside binding lectins that

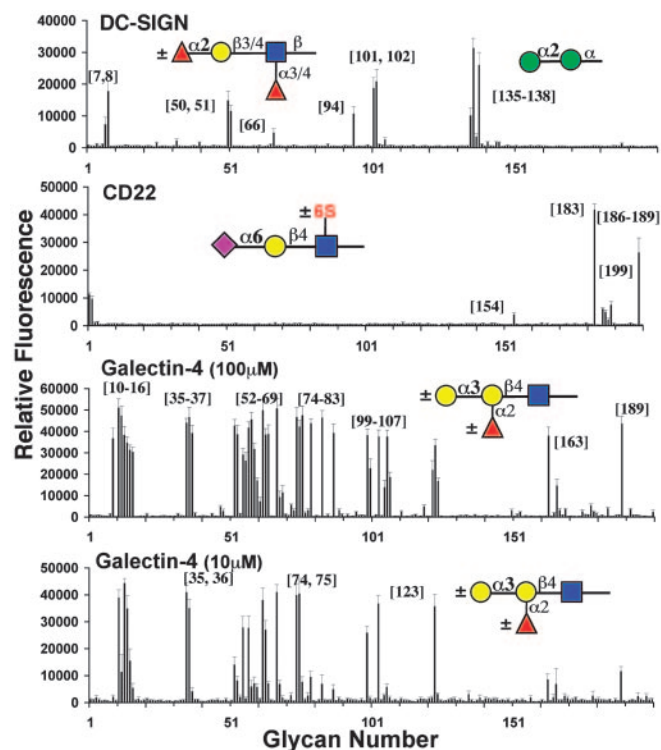


Fig. 4. Mammalian GBP specificity. C-type lectin (DC-SIGN): DC-SIGN-Fc chimera (30 $\mu\text{g/ml}$) detected by secondary goat anti-human-IgG-Alexa 488 antibody (10 $\mu\text{g/ml}$) bound selectively to $\alpha\text{1-2-}$ and/or $\alpha\text{1-3/4-}$ fucosylated glycans and to $\text{Man}\alpha\text{1-2}$ glycans. Siglec (CD22): CD22-Fc chimera (10 $\mu\text{g/ml}$) precomplexed with secondary goat anti-human-IgG-Alexa 488 (5 $\mu\text{g/ml}$) and tertiary rabbit anti-goat-IgG-FITC (2.5 $\mu\text{g/ml}$) antibodies bound exclusively to $\text{Neu5Ac}\alpha\text{2-6Gal-}$ glycans. Galectin (galectin-4): Human galectin-4-Alexa 488 (10 $\mu\text{g/ml}$) evaluated with glycans printed at 100 and 10 μM bound preferentially to blood group glycans.^m

bind terminal and internal galactose residues (46). Galectin-4 has been identified as a possible intracellular mediator with antiapoptotic activity (33, 47). By comparing galectin-4 binding to saturated glycans (printed at 100 μM concentration) with binding to subsaturated glycans (printed at 10 μM concentration), preferred binding specificities were revealed. In particular, $\text{Gal}\alpha\text{1-3-}$ linked to lactose (35–37), $\text{Fuc}\alpha\text{1-2-}$ linked to lac(NAc) (100, 103, and 105–107), or $\text{R-GlcNAc}\beta\text{1-3-}$ linked to lactose (123), as well as 3' sulfation (11–16), substantially enhanced the affinity. This specificity profile is similar to that reported for a rat ortholog of galectin-4 (48, 49).

Glycan-Specific Antibodies. We have analyzed monoclonal and polyclonal antiglycan antibodies from three different sources (Fig. 5). The commercial leukocyte differentiation antigen $\alpha\text{CD-15}$ has been documented to recognize a carbohydrate antigen, Lewis^x ($\text{Gal}\beta\text{1-4[Fu}\alpha\text{1-3]GlcNAc}$). When evaluated on the array it is highly specific for Lewis^x structures (7, 8, and 66) and does not recognize the same structure modified by additional sialylation (161), sulfation (26), fucosylation (102), or LacNAc extension (73). One of the most studied human anti-HIV mAbs is 2G12, which neutralizes a broad spectrum of natural HIV isolates via recognition of high mannose-type N-linked glycans on the major envelope glycoprotein, gp120 (27, 30, 31, 50, 51). The glycan array contains a variety of synthetic mannose fragments with the natural series of high mannose N-glycans (Man5-Man9) isolated from ribonuclease B. Recombinant 2G12 exhibited strong binding of synthetic $\text{Man}\alpha\text{1-2-terminal}$ mannose oligosaccharides (135, 136, and

^mSymbol structure insets represent the principal glycan structures recognized. See Fig. 2 for a complete list of structures.

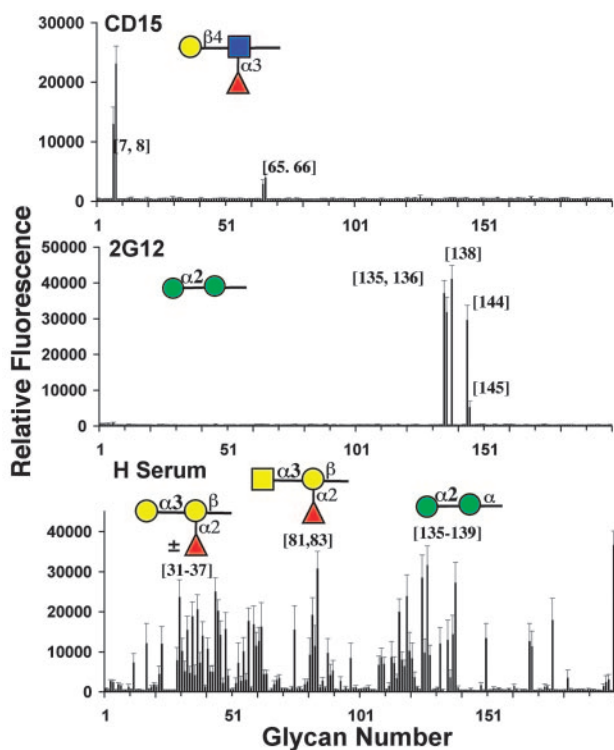


Fig. 5. Anticarbhydrate antibody specificity. (Top) Mouse anti-CD15-FITC mAb (BD Biosciences clone HI98, 100 tests) bound exclusively to Lewis^x glycans. (Middle) 2G12 mAb (30 μ g/ml) precomplexed with goat anti-human-IgG-FITC (15 μ g/ml) bound to specific Man α 1–2 glycans, including the Man8 and Man9 N-glycans. (Bottom) Human serum of 10 healthy individuals (1:25 dilution) was individually bound to glycan arrays and detected by subsequent overlay with monoclonal mouse anti-human-IgG-IgM-IgA-biotin antibody (10 μ g/ml) and streptavidin-FITC (10 μ g/ml). Results represent the mean and standard deviation for binding in all 10 experiments. Anticarbhydrate antibodies detecting various blood group antigens as well as mannans and bacterial fragments were found.^m

138) as observed previously (14, 27, 42). In addition, of the series of natural high mannose-type N-glycans, 2G12 exhibited preferred binding to Man8 glycans (144) relative to Man5, Man6, Man7, or Man9 glycans (140, 142, 143, and 145).

To test the array against more complex samples, antiglycan antibodies present in human serum were investigated. After incubation with serum, bound IgG, IgA, and IgM were detected by using labeled anti-human IgG/A/M antibody. A surprising diversity of antibody specificities was observed. It was remarkably consistent among samples from 10 individuals as indicated in Fig. 5. This profile of human antiglycan antibodies detects the ABO blood group fragments (variously represented in different individuals) (32, 81, and 83), mannose fragments (135–139), α -Gal- (31–37), and ganglioside-epitopes (55–59, 132, and 168), as well as fragments of the Gram-negative bacterial cell wall peptidoglycan (127) and rhamnose (200). Notably, glycans containing the Gal β 1–3GlcNAc substructure were consistently detected (12, 61, 62, 132, 150, and 168) except when fucosylated (25, 51, 94, and 100), thus generating the human blood group antigens H, Lewis^a or Lewis^b. All of these structures can be identified as either blood group antigens or fragments of microorganisms (e.g., bacteria, yeast, etc.) to which humans are exposed.

Analysis of Bacterial and Viral GBPs. CVN is a cyanobacterial protein that can block the initial step of HIV-1 infection by binding to high mannose groups on the envelope glycoprotein

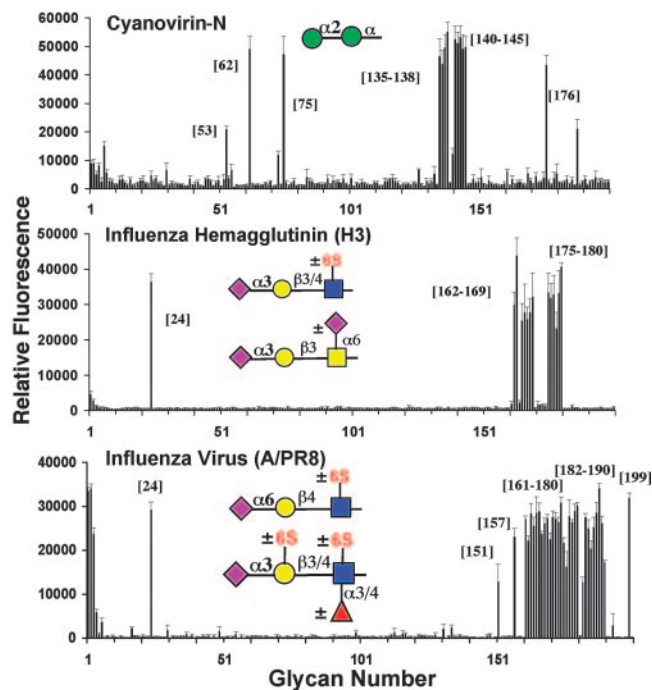


Fig. 6. Bacterial and viral GBP specificity. (Top) CVN (30 μ g/ml) detected with secondary polyclonal rabbit anti-CVN (10 μ g/ml) and tertiary anti-rabbit-IgG-FITC (10 μ g/ml) bound various α 1–2 mannosides. (Middle) Pure recombinant hemagglutinin (150 μ g/ml) derived from duck/Ukraine/1/63 (H3/N7), precomplexed with mouse anti-HisTag-IgG-Alexa 488 (75 μ g/ml) and anti-mouse-IgG-Alexa 488 (35 μ g/ml), bound exclusively to Neu5Aca2–3Gal-terminating glycans. (Bottom) Intact influenza virus A/Puerto Rico/8/34 (H1N1) was applied at 100 μ g/ml in the presence of 10 μ M of the neuraminidase inhibitor oseltamivir carboxylate. The virus bound a wide spectrum of sialosides with both NeuAca2–3Gal and NeuAca2–6Gal sequences.^m

gp120 (42, 52). On the array, CVN specifically recognized the synthetic fragments bearing terminal Man α 1–2- residues (135–138), as well as high mannose glycans with one or more Man α 1–2- termini (140–145), in keeping with its reported specificity (Fig. 6). In addition, CVN bound to several lacto- and neolacto- structures (53, 62, 75, and 176).

Influenza viruses exhibit specificity in their ability to recognize sialosides as cell surface receptor determinants through the viral binding protein, the hemagglutinin. Depending on the species of origin, the hemagglutinin has specificity for sialosides with sialic acid in the NeuAca2–3Gal or NeuAca2–6Gal linkage (53–55). While the intrinsic affinity of sialosides for the hemagglutinin is weak ($K_d \approx 2$ mM), binding is strengthened through polyvalent interactions at the cell surface (56). Results shown in Fig. 6 reveal the binding of a recombinant avian H3 hemagglutinin (duck/Ukraine/1/63) bound to Neu5Aca2–3-linked to galactosides (24, 162–169, and 176–180), but not to any Neu5Aca2–6- or Neu5Aca2–8- linked sialosides. Intact influenza viruses, such as A/Puerto Rico/8/34 (H1N1), were also strongly bound to the array. The overall affinities are consistent with previous findings and show specificity for both a2–3 and a2–6 sialosides (57). Detailed fine specificities were also revealed such as binding to Neu5Aca2–3- and Neu5Aca2–6- linked to galactosides (24, 151, 157, 161–180, 182–190, and 199), as well as certain O-linked sialosides.

Discussion

The glycan microarray presented in this article uses standard robotic printing, scanning, and image analysis software used for

DNA microarrays. The combination of using amine-functionalized glycans with the NHS-activated glass surface results in robust and reproducible covalent attachment of glycans with no modifications of standard DNA printing protocols. The array can be used with no further preparation of the surface for assessing the specificity of a wide variety of GBPs, yielding uniformly low backgrounds regardless of the labeled protein used for detection. Moreover, only 0.1–2 μg of GBP is needed for optimal signal, >100-fold less than required for our ELISA-based array that uses predominately the same glycan library.¹¹ The array performed well for a wide variety of GBPs, confirming primary specificities documented by other means, and revealing unique aspects of fine specificity not previously recognized.

It is noteworthy that substantial signal enhancement is achieved for GBPs on the array when multivalent displays of the glycan binding domain are used (Table 1). This effect reflects the low intrinsic affinity of GBPs for their preferred glycan ligands, with typical K_d values of 1–1,000 μM (36). In general, multivalent display of the GBPs will tend to amplify differences of specificity relative to the intrinsic affinities and reveal biologically important specificities. As a case in point, the difference in intrinsic affinities of influenza virus H3 hemagglutinin for $\alpha 2\text{--}3$ and $\alpha 2\text{--}6$ sialosides is only 2-fold, yet multivalent display of hemagglutinins amplify the difference to 100- to 1,000-fold for specific adsorption of the virus to cell surfaces bearing the preferred sequence (53, 56).

The importance of valency extends to comparing specificities of GBPs obtained by using different assays. In the case of DC-SIGN, the dual specificities for mannose-containing glycans and fucose-

containing glycans (including Lewis^x and Lewis^a structures) observed previously (8), were also observed here. However, the binding of the series of natural branched high mannose-containing N-glycans (142–145) was low in the present study and nearly equal to that of the fucosides in the study by Guo *et al.* (8). This apparent discrepancy may be related to the differences in the multivalent presentation of the GBP (dimeric Fc chimera vs. renatured tetramer), the presentation of the oligosaccharide, or both. In this study we have saturated the surface of the NHS-derivatized glass with glycan to similar density as evidenced by the binding of Con A (Fig. 3). In the Guo *et al.* study, biotinylated glycans were adsorbed to streptavidin-coated wells of an ELISA plate, providing a lower uniform density of tetrameric streptavidin binding up to four oligosaccharides.

In addition to the utility of the glycan array for analysis of GBP specificity, this system has potential in therapeutic developments. A striking result is the ability to reproducibly detect a variety of antiglycan antibody specificities in crude human serum. This finding raises the possibility of the use of the array in screening for glycan-specific antibodies with potential for diagnosis in patients with microbial infections, cancer, and autoimmune disease or after xenotransplantation.

We thank various sponsors (see www.functionalglycomics.org/static/consortium/sponsors.shtml) and numerous investigators for contributing enzyme constructs and other reagents that have been used in the synthesis of the glycan library. We thank Dr. Ajit Varki (University of California at San Diego, La Jolla) for providing the human CD22 construct and Anna Tran-Crie and Matthew Fowler for help in preparing this manuscript. The influenza neuraminidase inhibitor oseltamivir carboxylate was a gift from Hoffmann–La Roche. This work was supported by National Institute of General Medical Sciences Grant GM62116 to the Consortium for Functional Glycomics.

¹¹The array using the ELISA format uses biotinylated glycans adsorbed to streptavidin. It is currently available for use by investigators through the Consortium for Functional Glycomics (www.functionalglycomics.org) and soon will be replaced by the printed microarray described here.

- Hakomori, S.-I. (2001) in *The Molecular Immunology of Complex Carbohydrates-2*, ed. Wu, A. M. (Plenum, New York), pp. 369–402.
- Taylor, M. E. & Drickamer, K. (2003) *Introduction to Glycobiology* (Oxford Univ. Press, Oxford).
- Mrksich, M. (2004) *Chem. Biol.* **11**, 739–740.
- Feizi, T., Fazio, F., Wengang, C. & Wong, C.-H. (2003) *Curr. Opin. Struct. Biol.* **13**, 637–645.
- Drickamer, K. & Taylor, M. E. (2002) *Genome Biology* **3**, 1034.1–1034.4.
- Love, K. R. & Seeberger, P. H. (2002) *Angew. Chem. Int. Ed.* **41**, 3583–3586.
- Galanina, O. E., Mecklenburg, M., Nifantiev, N. E., Pazylnina, G. V. & Bovin, N. V. (2004) *Lab. Chip.* **3**, 260–265.
- Guo, Y., Feinberg, H., Conroy, E., Mitchell, D. A., Alvarez, R., Blixt, O., Taylor, M. E., Weis, W. I. & Drickamer, K. (2004) *Nat. Struct. Mol. Biol.* **11**, 591–598.
- Wang, D., Liu, S., Trummer, B. J., Deng, C. & Wang, A. (2002) *Nat. Biotechnol.* **20**, 275–281.
- Fukui, S., Feizi, T., Galustian, C., Lawson, A. M. & Chai, W. (2002) *Nat. Biotechnol.* **20**, 1011–1017.
- Willats, W. G. T., Rasmussen, S. E., Kristensen, T., Mikkelsen, J. D. & Knox, J. P. (2002) *Proteomics* **2**, 1666–1671.
- Fazio, F., Bryan, M. C., Blixt, O., Paulson, J. C. & Wong, C.-H. (2002) *J. Am. Chem. Soc.* **124**, 14397–14402.
- Nimrichter, L., Gargir, A., Gortler, M., Alstock, R. T., Shtevi, A., Weissshaus, O., Fire, E., Dotan, N. & Schnaar, R. L. (2004) *Glycobiology* **14**, 197–203.
- Bryan, M. C., Fazio, F., Lee, H. K., Huang, C. Y., Chang, A. Y., Best, M. D., Calarese, D. A., Blixt, O., Paulson, J. C., Burton, D. R., *et al.* (2004) *J. Am. Chem. Soc.* **126**, 8640–8641.
- Park, S., Lee, M. R., Pyo, S. J. & Shin, I. (2004) *J. Am. Chem. Soc.* **126**, 4812–4819.
- Ratner, D. M., Adams, E. W., Su, J., O'Keefe, B. R., Mrksich, M. & Seeberger, P. H. (2004) *ChemBiochemistry* **5**, 379–382.
- Schwarz, M., Spector, L., Gargir, A., Shtevi, A., Gortler, M., Alstock, R. T., Dukler, A. A. & Dotan, N. (2003) *Glycobiology* **13**, 749–754.
- Houseman, B. T. & Mrksich, M. (2002) *Chem. Biol.* **9**, 443–454.
- Pazylnina, G. V. & Shin, I. (2002) *Angew. Chem. Int. Ed.* **41**, 3180–3182.
- Bergh, A., Magnusson, B. G., Ohlsson, J., Wellmar, U. & Nilsson, U. J. (2001) *Glycoconj. J.* **18**, 615–621.
- Shiyan, S. D. & Bovin, N. V. (1997) *Glycoconj. J.* **14**, 631–638.
- Pazylnina, G. V., Sablina, M. A., Tuzikov, A. B., Chinarev, A. A. & Bovin, N. V. (2003) *Mendeleev Commun.* **13**, 245–248.
- Pazylnina, G. V., Tyrtysht, T. V. & Bovin, N. V. (2002) *Mendeleev Commun.* **12**, 183–184.
- Pazylnina, G. V., Tuzikov, A. B., Chinarev, A. A., Obukhova, P. & Bovin, N. V. (2002) *Tetrahedron Lett.* **43**, 8011–8013.
- Nifant'ev, N. E., Tsvetkov, Y. E., Shashkov, A. S., Kononov, L. O., Menshov, V. M., Tuzikov, A. B. & Bovin, N. V. (1996) *J. Carbohydr. Chem.* **15**, 939–953.
- Zemlyanukhina, T. V., Nifant'ev, N. E., Shashkov, A. S., Tsvetkov, Y. E. & Bovin, N. V. (1995) *Carbohydr. Lett.* **1**, 277–284.
- Lee, H. K., Scanlan, C. N., Huang, C. Y., Chang, A. Y., Calarese, D. A., Dwek, R. A., Rudd, P. M., Burton, D. R., Wilson, I. A. & Wong, C. H. (2004) *Angew. Chem. Int. Ed.* **43**, 1000–1003.
- van Die, I., van Vliet, S. J., Nyame, A. K., Cummings, R. D., Bank, C. M. C., Appelmelk, B. J., Geijtenbeek, T. B. & Kooyk, Y. (2003) *Glycobiology* **13**, 471–478.
- Gamblin, S. J., Haire, L. F., Russell, R. J., Stevens, D. J., Xiao, B., Ha, Y., Vasishth, N., Steinhauer, D. A., Daniels, R. S., Elliot, A., *et al.* (2004) *Science* **303**, 1838–1842.
- Calarese, D. A., Scanlan, C. N., Zwirk, M. B., Deechongkit, S., Mimura, Y., Kunert, R., Zhu, P., Wormald, M. R., Stanfield, R. L., Roux, K. H., *et al.* (2003) *Science* **300**, 2065–2071.
- Scanlan, C. N., Pantophlet, R., Wormald, M. R., Ollmann Saphire, E., Stanfield, R., Wilson, I. A., Katinger, H., Dwek, R. A., Rudd, P. M. & Burton, D. R. (2002) *J. Virol.* **76**, 7306–7321.
- Blixt, O., Collins, B. E., van den Nieuwenhof, I. M., Crocker, P. R. & Paulson, J. C. (2003) *J. Biol. Chem.* **278**, 31007–31019.
- Huflejt, M. E., Jordan, E. T., Gitt, M. A., Barondes, S. H. & Leffler, H. (1997) *J. Biol. Chem.* **272**, 14294–14303.
- Ting, C. A., Lee, S.-F. & Wang, K. (2003) *BioTechniques* **35**, 808–810.
- Blixt, O. & Razi, N. (2004) in *Synthesis of Carbohydrates Through Biotechnology*, eds. Wang, P. G. & Ichikawa, Y. (Am. Chem. Soc., Washington, DC), Vol. 873, pp. 93–112.
- Collins, B. E. & Paulson, J. C. (2004) *Curr. Opin. Chem. Biol.* **8**, 617–625.
- Gupta, D., Oscarson, S., Raju, T. S., Stanely, P., Toone, E. J. & Brewer, C. F. (1996) *Eur. J. Biochem.* **242**, 320–326.
- Brewer, F., Bhattacharyya, L., Brown, R. D. & Koenig, S. H. (1985) *Biochem. Biophys. Res. Commun.* **127**, 1066–1071.
- Lis, H. & Sharon, N. (1987) *Methods Enzymol.* **138**, 544–551.
- Iglesias, J. L., Lis, H. & Sharon, N. (1982) *Eur. J. Biochem.* **123**, 247–252.
- Kooyk, Y. & Geijtenbeek, T. B. (2002) *Immunol. Rev.* **186**, 47–56.
- Adams, E. W., Ratner, D. M., Bokesch, H. R., McMahon, J. B., O'Keefe, B. R. & Seeberger, P. H. (2004) *Chem. Biol.* **11**, 875–881.
- Engel, P., Nojima, Y., Rothstein, D., Zhou, L. J., Wilson, G. L., Kehrl, J. H. & Tedder, T. F. (1993) *J. Immunol.* **150**, 4719–4732.
- Kelm, S., Pelz, A., Schauer, R., Filbin, M. T., Tang, S., de Bellard, M. E., Schnaar, R. L., Mahoney, J. A., Hartnell, A., Bradfield, P. & Crocker, P. R. (1994) *Curr. Biol.* **4**, 965–972.
- Powell, L. D., Sgroi, D., Sjoberg, E. R., Stamenkovic, I. & Varki, A. (1993) *J. Biol. Chem.* **268**, 7019–7027.
- Hirabayashi, J., Hashidate, T., Arata, Y., Nishi, N., Nakamura, T., Hirashima, M., Urashima, T., Oka, T., Futai, M., Muller, W. E., *et al.* (2002) *Biochim. Biophys. Acta* **1572**, 232–254.
- Huflejt, M. E. & Leffler, H. (2004) *Glycoconj. J.* **20**, 247–255.
- Wu, A. M., Wu, J. H., Liu, J. H., Singh, T., Andre, S., Kaltner, H. & Gabius, H. J. (2004) *Biochimie* **86**, 317–326.
- Oda, Y., Herrmann, J., Gitt, M. A., Turck, C. W., Burlingame, A. L., Barondes, S. H. & Leffler, H. (1993) *J. Biol. Chem.* **268**, 5929–5939.
- Sanders, R. W., Venturi, M., Schiffler, L., Kalyanaraman, R., Katinger, H., Lloyd, K. O., Kwong, P. D. & Moore, J. P. (2002) *J. Virol.* **76**, 7293–7305.
- Trkola, A., Purtscher, M., Muster, T., Ballaun, C., Buchacher, A., Sullivan, N., Srinivasan, K., Sodroski, J., Moore, J. P. & Katinger, H. (1996) *J. Virol.* **70**, 1100–1108.
- Bewely, C. A. & Otero-Quintero, S. (2001) *J. Am. Chem. Soc.* **123**, 3892–3902.
- Connor, R. J., Kawaoka, Y., Webster, R. G. & Paulson, J. C. (1994) *Virology* **205**, 17–23.
- Rogers, G. N. & D'Souza, B. L. (1989) *Virology* **173**, 317–322.
- Rogers, G. N., Paulson, J. C., Daniels, R. S., Skehel, J. J., Wilson, I. A. & Wiley, D. C. (1983) *Nature* **304**, 76–78.
- Sauter, N. K., Bednarski, M. D., Wurzburg, B. A., Hanson, J. E., Whitesides, G. M., Skehel, J. J. & Wiley, D. C. (1989) *Biochemistry* **28**, 8388–8396.
- Rogers, G. N. & Paulson, J. C. (1983) *Virology* **127**, 361–373.